BornAgain

Incomplete Physics Manual

Software version 1.16

This document last updated April 10, 2020

Marina Ganeva, Gennady Pospelov, Walter Van Herck, Joachim Wuttke

Scientific Computing Group
Jülich Centre for Neutron Science
at Heinz Maier-Leibnitz Zentrum Garching
Forschungszentrum Jülich GmbH

Homepage: http://www.bornagainproject.org

Authors: Marina Ganeva, Gennady Pospelov, Walter Van Herck, Joachim Wuttke

Scientific Computing Group

at Heinz Maier-Leibnitz Zentrum (MLZ) Garching

Disclaimer: Software and documentation are work in progress.

We cannot guarantee correctness and accuracy.

If in doubt, contact us for assistance or scientific collaboration.

Funding: This project has received funding from the European Union's Horizon 2020 research and innovation programme under grant agreement No 654000.

Contents

Preface

About BornAgain

BornAgain is a software package to simulate and fit reflectometry, off-specular scattering, and grazing-incidence small-angle scattering (GISAS) of X-rays and neutrons. It provides a generic framework for modeling multilayer samples with smooth or rough interfaces and with various types of embedded nanoparticles. The name, BornAgain, alludes to the central role of the distorted-wave Born approximation (DWBA) in the physical description of the scattering process.

BornAgain is maintained by the Scientific Computing Group of the Jülich Centre for Neutron Science (JCNS) at Heinz Maier-Leibnitz Zentrum (MLZ) Garching, Germany. It free and open source software. The source code is released under the GNU General Public License (GPL, version 3 or higher), the documentation under the Creative Commons license CC-BY-SA.

This manual vs other documentation

This Physics Manual explains some of the theory behind BornAgain. It is restricted to topics that are not covered by other components of the BornAgain documentation. These include:

- Our 2020 article in J. Appl. Cryst. [1] that gives a broad overview over BornAgain. The implemented physics is summarized in Sect. 5.
- The web site `https://www.bornagainproject.org`, which includes instructions how to download and install BornAgain, and extensive tutorials on setting up physical models.
- The complete documentation of the Application Programming Interface (API), which can be generated by running the open-source tool *Doxygen* over the source code.
- Further technical documents, available from the *Documents* tab on the download page. So far, there exists one such document, namely the Form factor catalog.

This Physics Manual is work in progress. In future editions, it may grow as we elaborate details or add new chapters, but it may also shrink as we move contents to journal articles or other documents.

Citation

The canonical reference for BornAgain is the journal article [1]

> Gennady Pospelov, Walter Van Herck, Jan Burle, Juan M. Carmona Loaiza, Céline Durniak, Jonathan M. Fisher, Marina Ganeva, Dmitry Yurov and Joachim Wuttke:
> BornAgain: software for simulating and fitting grazing-incidence small-angle scattering
> J. Appl. Cryst. 53, 262–276 (2020)

Use of the software should additionally be documented by citing a specific version thereof:

> BornAgain — Software for simulating and fitting X-ray and neutron small-angle scattering at grazing incidence, version ⟨`version`⟩ (⟨`release date`⟩), `http://www.bornagainproject.org`

Citation of the present Physics Manual is only necessary when referring to specific information. As this document is subject to frequent and substantial change, it is important to refer to a specific edition by indicating the release date printed on the title page:

> Marina Ganeva, Gennady Pospelov, Walter Van Herck, Joachim Wuttke:
> BornAgain Physics Manual (⟨`release date`⟩),
> `http://www.bornagainproject.org`

Old editions can be retrieved from the BornAgain source repository.

The initial design of BornAgain and much of the implemented physics owe much to the widely used program IsGISAXS by Rémi Lazzari [2]. Depending on how BornAgain is used in scientific work, it may be appropriate to cite the pioneering papers by Lazzari *et al.* [3, 4].

Typographic Conventions

We use the following colored boxes to highlight certain information:

Such a box contains a **warning** about potential problems with the software or the documentation.

This road sign in the margin indicates **work in progress**.

An **implementation note** explains how the theory exposed in this manual is actually used in BornAgain.

This is a link.

Mathematical notations are explained in the symbol index, page Y:1. Snomencl

This document is formatted for single-sided printing, which is more convenient for reading on a screen.

1 Scattering

This chapter provides a self-contained introduction into the theory of neutron and X-ray scattering, as needed for the analysis of grazing-incidence small-angle scattering (GISAS) experiments. In Section 1.1, a generic wave equation is derived. In Section 1.3, it is solved in first-order distorted-wave Born approximation (DWBA). The chapter finishes with a qualitative discussion of coherence lengths in Section 1.4.

1.1 Wave propagation

In this section, we review the wave equations that describe the propagation of neutrons (Secs. 1.1.1 and 1.1.2) and X-rays (Sec. 1.1.3) in matter, and combine them into a unified wave equation (Sec. 1.1.4) that is the base for the all following analysis. This provides justification and background for Eqns. 1–3 in the BornAgain reference paper [1].

1.1.1 Neutrons in a scalar potential

The scalar wavefunction $\psi(\boldsymbol{r},t)$ of a free neutron in absence of a magnetic field is governed by the Schrödinger equation

$$i\hbar\partial_t\psi(\boldsymbol{r},t)=\left[-\frac{\hbar^2}{2m}\boldsymbol{\nabla}^2+V(\boldsymbol{r})\right]\psi(\boldsymbol{r},t). \tag{1.1}$$ {EQSchrodi1}

BornAgain concentrates on elastic scattering; inelastic scattering is either neglected, or accounted for by some extra damping as discussed at the end of this subsection. Therefore, any time dependence of the potential $V(\boldsymbol{r}) \coloneqq \langle V(\boldsymbol{r},t)\rangle$ is averaged out, and only monochromatic waves with given frequency ω are considered. In consequence, the wavefunction

$$\psi(\boldsymbol{r},t)=\psi(\boldsymbol{r})\mathrm{e}^{-i\omega t} \tag{1.2}$$ {Estationarywave}

factorizes into a stationary wave and a time-dependent phase factor. In the following, we will characterize the incoming radiation not by its energy $\hbar\omega$, but by its *vacuum wavenumber* K, given by the dispersion relation

$$\hbar\omega=\frac{(\hbar K)^2}{2m}. \tag{1.3}$$

We rescale the potential as

$$v(\boldsymbol{r}) \coloneqq \frac{2m}{\hbar^2} V(\boldsymbol{r}). \tag{1.4}$$

This deviates by a factor 4π from our previous choice in [1]. The Schrödinger equation (1.1) now takes the simple form

$$\left[\boldsymbol{\nabla}^2 + K^2 - v(\boldsymbol{r})\right] \psi(\boldsymbol{r}) = 0. \tag{1.5}$$

The microscopic expression for $v(\boldsymbol{r})$ is based on Fermi's pseudopotential,

$$v(\boldsymbol{r}) = 4\pi \sum_j \left\langle b_j \delta\left(\boldsymbol{r} - \boldsymbol{r}_j(t)\right)\right\rangle. \tag{1.6}$$

The sum runs over all nuclei in the scattering target. The *bound scattering length* b_j is isotope specific; values are tabulated [5].

In small-angle scattering, as elsewhere in neutron optics [6], the potential (1.6) can be coarse-grained by spatially averaging over at least a few atomic diameters, yielding the *scattering length density* (SLD) [6, eq. 2.8.37].

$$v(\boldsymbol{r}) = \sum_s b_s \rho_s(\boldsymbol{r}). \tag{1.7}$$

Here the sum runs over chemical elements, $b_s \coloneqq \langle b_j \rangle_{j \in s}$ is the bound *coherent* scattering length, and ρ_s is a number density.

In passing from (1.6) to (1.7), we neglected Bragg scattering from atomic-scale correlation, and incoherent scattering from spin or isotope related fluctuations of b_j. In small-angle experiments, incoherent scattering only contributes a diffuse background. Furthermore, it is possible that it causes a noticeable attenuation of the incoming or scattered radiation. Other loss channels are elastic wide-angle scattering and inelastic scattering. They can all be lumped into an ad-hoc increment of the imaginary part of the refractive index, which otherwise, at the microscopic level (1.6), accounts for absorption only. Furthermore, incoherent scattering, as inelastic scattering, contributes to the diffuse background in the detector.

1.1.2 Neutrons in a magnetic field

In the presence of a magnetic field, the propagation of free neutrons becomes spin dependent. Therefore the scalar wavefunction of Sec. 1.1.1 must be replaced by a spinor $\boldsymbol{\Psi}$. The magnetic moment $\boldsymbol{\mu}$ of the neutron couples to the magnetic induction $\boldsymbol{B}$ [6, 7, 8]. With the Pauli vector $\boldsymbol{\sigma}$, composed of the three Pauli matrices, the interaction can be written

$$V_{\text{magn}} = -\boldsymbol{\mu}\boldsymbol{B} = +\mu\boldsymbol{\sigma}\boldsymbol{B}. \tag{1.8}$$

The final expression has a plus sign because the magnetic moment of the neutron is antiparallel to its spin, as expressed by the gyromagnetic ratio -1.91. We introduce the reduced field

$$\boldsymbol{b} \coloneqq \frac{2m\mu}{\hbar^2} \boldsymbol{B}, \tag{1.9}$$

to write the spin-dependent Schrödinger equation as

$$\left[\boldsymbol{\nabla}^2 + K^2 - v(\boldsymbol{r}) - \boldsymbol{b}(\boldsymbol{r})\boldsymbol{\sigma}\right]\boldsymbol{\Psi}(\boldsymbol{r}) = 0. \tag{1.10}$$

{ESchwedi2H}

1.1.3 X-rays

The propagation of X-rays is governed by Maxwell's equations. We shall use SI units throughout:

$$\begin{aligned}\boldsymbol{\nabla}\times\boldsymbol{E} &= -\partial_t\boldsymbol{B}, \quad \boldsymbol{\nabla}\boldsymbol{B} = 0, \quad \boldsymbol{B} = \boldsymbol{\mu}(\boldsymbol{r})\mu_0\boldsymbol{H},\\ \boldsymbol{\nabla}\times\boldsymbol{H} &= +\partial_t\boldsymbol{D}, \quad \boldsymbol{\nabla}\boldsymbol{D} = 0, \quad \boldsymbol{D} = \boldsymbol{\epsilon}(\boldsymbol{r})\epsilon_0\boldsymbol{E}.\end{aligned} \tag{1.11}$$

{EMaxwellII}

Since BornAgain only addresses elastic scattering, we assume the permeability and permittivity tensors $\boldsymbol{\mu}$ and $\boldsymbol{\epsilon}$ to be time-independent. Therefore we only consider monochromatic waves with given frequency ω,

$$\boldsymbol{E}(\boldsymbol{r},t) = \boldsymbol{E}(\boldsymbol{r})\mathrm{e}^{-i\omega t}, \tag{1.12}$$

{EstationaryX}

and similarly for the other fields $\boldsymbol{D}$, $\boldsymbol{H}$, $\boldsymbol{B}$. The minus sign in the exponent has been chosen for consistency with the neutron case (1.2), where it is an inevitable consequence of the standard form of the Schrödinger equation. Opposite to this *quantum-mechanical convention*, there exists a *crystallographic convention*, which is preferred in most texts on X-ray crystallography, including influential texts on GISAXS [4].

ReLL09

Since magnetic refraction or scattering is beyond the scope of BornAgain, the relative magnetic permeability tensor is always $\boldsymbol{\mu}(\boldsymbol{r}) = 1$. As customary in SAXS and GISAXS, we assume that the dielectric properties of the material are those of a polarizable electron cloud. This is occasionally called the *Laue model* [9]. Thereby the relative dielectric permittivity tensor $\boldsymbol{\epsilon}$ becomes a scalar,

Lau31

$$\epsilon(\boldsymbol{r}) = 1 - \frac{4\pi r_e}{K^2}\rho(\boldsymbol{r}), \tag{1.13}$$

with the classical electron radius $r_e = e^2/(4\pi\epsilon_0 mc^2) \simeq 2.8\cdot 10^{-15}$ m, the electron number density $\rho(\boldsymbol{r})$, and the vacuum wavenumber K, given by the dispersion relation

$$K^2 = \mu_0\epsilon_0\omega^2 = \omega^2/c^2. \tag{1.14}$$

With these simplifying assumptions about $\boldsymbol{\epsilon}$ and $\boldsymbol{\mu}$, Maxwell's equations yield the wave equation

$$\boldsymbol{\nabla}\times\boldsymbol{\nabla}\times\boldsymbol{E} = K^2\epsilon(\boldsymbol{r})\boldsymbol{E}. \tag{1.15}$$

{ENabCrossNabE}

Using a standard identity from vector analysis, it can be brought into the more tractable form

$$\left[\boldsymbol{\nabla}^2 - \boldsymbol{\nabla}\otimes\boldsymbol{\nabla} + K^2\epsilon(\boldsymbol{r})\right]\boldsymbol{E}(\boldsymbol{r}) = 0. \tag{1.16}$$

{ENabNabE}

1.1.4 Unified wave equation

We combine all the above in a unified wave equation

$$[\boldsymbol{D}_0 - \boldsymbol{V}(\boldsymbol{r})]\,\boldsymbol{\Psi}(\boldsymbol{r}) = 0 \tag{1.17}$$ {EWAVE}

with the vacuum wave operator

$$\boldsymbol{D}_0 \coloneqq \begin{cases} \boldsymbol{\nabla}^2 + K^2 & \text{for neutrons,} \\ \boldsymbol{\nabla}^2 - \boldsymbol{\nabla} \otimes \boldsymbol{\nabla} + K^2 & \text{for X-rays} \end{cases} \tag{1.18}$$ {EDo}

and the potential

$$\boldsymbol{V}(\boldsymbol{r}) \coloneqq \begin{cases} v(\boldsymbol{r}) & \text{for neutrons (scalar),} \\ v(\boldsymbol{r}) + \boldsymbol{b}(\boldsymbol{r})\boldsymbol{\sigma} & \text{for neutrons (spinorial),} \\ K^2(\epsilon(\boldsymbol{r}) - 1) & \text{for X-rays.} \end{cases} \tag{1.19}$$ {ETV}

The generic wave amplitude $\boldsymbol{\Psi}$ shall represent the scalar neutron wavefunction ψ, the spinor $\boldsymbol{\Psi}$, or the electric vector field $\boldsymbol{E}$, as applicable.

1.1.5 Flux

In quantum mechanics, the current density, or flux, is

$$\langle \boldsymbol{J} \rangle = \langle \boldsymbol{\Psi} | \, \frac{|\boldsymbol{r}\rangle \langle \boldsymbol{r}| \, \boldsymbol{k} + \boldsymbol{k} \, |\boldsymbol{r}\rangle \langle \boldsymbol{r}|}{2} \, | \boldsymbol{\Psi} \rangle \, . \tag{1.20}$$ {EdefJop}

The electromagnetic energy flux is given by the Poynting vector,

$$\boldsymbol{S} \coloneqq \mathrm{Re}(\boldsymbol{E}(\boldsymbol{r}, t)) \times \mathrm{Re}(\boldsymbol{H}(\boldsymbol{r}, t)). \tag{1.21}$$

In both cases, the flux is proportional to the squared modulus of the wave amplitude,

$$J \propto |\boldsymbol{\Psi}(\boldsymbol{r})|^2. \tag{1.22}$$ {EFLUX}

Prefactors are ignorable as they cancel under the normalization of the scattered to the incoming flux.

1.2 Scattering in Born approximation

Most neutron and X-ray diffraction experiments are adequately described as plane-wave scattering in first order Born approximation. This is not the case for the grazing-incidence experiments addressed by BornAgain. Nonetheless, for the clarity of exposition, in this section we review the standard plane-wave scattering theory, before in the next section we turn to distorted waves.

1.2.1 Born approximation

In function-space notation, the perturbed wave equation (1.17) reads

$$(\boldsymbol{D}_0 - \boldsymbol{V})\,|\boldsymbol{\Psi}\rangle = 0. \tag{1.23}$$ {E1Wave3}

Choose an incident plane wave $\boldsymbol{\Phi}_\mathrm{i}$ that solves (1.23) in vacuum ($\boldsymbol{V} = 0$). With the Green function

$$\boldsymbol{G}_0 \coloneqq \boldsymbol{D}_0^{-1} \tag{1.24}$$ {EdefG}

we can transform (1.23) into a Lippmann-Schwinger equation,

$$|\boldsymbol{\Psi}\rangle = |\boldsymbol{\Phi}_\mathrm{i}\rangle + \boldsymbol{G}_0\boldsymbol{V}\,|\boldsymbol{\Psi}\rangle\,. \tag{1.25}$$ {E1LS3}

Operate on both sides from the left with $\boldsymbol{D}_0$ to see how this equation reduces to (1.23).

The Lippmann-Schwinger equation can be resolved by iterative substitution into an infinite series,

$$|\boldsymbol{\Psi}\rangle = |\boldsymbol{\Phi}_\mathrm{i}\rangle + \boldsymbol{G}_0\boldsymbol{V}\,|\boldsymbol{\Phi}_\mathrm{i}\rangle + \boldsymbol{G}_0\boldsymbol{V}\boldsymbol{G}_0\boldsymbol{V}\,|\boldsymbol{\Phi}_\mathrm{i}\rangle + \ldots \tag{1.26}$$ {E1BornSeries}

This is the *Born expansion* or *Born series*.[1] In *first-order Born approximation*, only the linear order in $\boldsymbol{V}$ is retained,

$$|\boldsymbol{\Psi}\rangle = (1 + \boldsymbol{G}_0\boldsymbol{V})\,|\boldsymbol{\Phi}_\mathrm{i}\rangle\,. \tag{1.27}$$ {E1Born1}

In scattering experiments we are only interested in the scattered wave at positions $\boldsymbol{r}$ that are far away from the sample ($r \to \infty$) and that are not illuminated by the distorted (refracted or reflected) incident beam,

$$|\boldsymbol{\Psi}_\mathrm{s}^\infty\rangle \coloneqq \boldsymbol{G}_0^\infty\boldsymbol{V}\,|\boldsymbol{\Phi}_\mathrm{i}\rangle\,. \tag{1.28}$$ {E1BornS}

Spelled out in real-space representation,

$$\boldsymbol{\Psi}_\mathrm{s}^\infty(\boldsymbol{r}) = \int \mathrm{d}^3r'\,\boldsymbol{G}_0^\infty(\boldsymbol{r},\boldsymbol{r}')\boldsymbol{V}(\boldsymbol{r}')\boldsymbol{\Phi}_\mathrm{i}(\boldsymbol{r}'). \tag{1.29}$$ {E1PsiS}

To proceed further, we need the far-field Green function $\boldsymbol{G}_0^\infty$.

[1] Named after Max Born who introduced it in quantum mechanics. It is actually due to Lord Rayleigh who devised it for sound, and later also applied it to electromagnetic waves, which resulted in his famous explanation of the blue sky.

1.2.2 Vacuum Green function

The retarded Green function describes the propagation of radiation that emanates from a point source. The retarded vacuum Green function $\boldsymbol{G}_0$ obyes the differential equation

$$\boldsymbol{D}_0\boldsymbol{G}_0(\boldsymbol{r},\boldsymbol{r}') = \mathbf{1}\delta(\boldsymbol{r}-\boldsymbol{r}'), \tag{1.30}$$ {EdefGo}

plus a boundary condition to ensure that the solution is an *outgoing* wave. We write a scalar outgoing spherical wave as

$$g(r) \coloneqq \frac{\mathrm{e}^{iKr}}{4\pi r}. \tag{1.31}$$ {Egr}

The retarded vacuum Green function is then

$$\boldsymbol{G}_0(\boldsymbol{r},\boldsymbol{r}') = \begin{cases} g(|\boldsymbol{r}-\boldsymbol{r}'|) & \text{for neutrons (scalar),} \\ \mathbf{1}g(|\boldsymbol{r}-\boldsymbol{r}'|) & \text{for neutrons (spinorial),} \\ (\mathbf{1}+K^{-2}\boldsymbol{\nabla}\otimes\boldsymbol{\nabla})g(|\boldsymbol{r}-\boldsymbol{r}'|) & \text{for X-rays [13].} \end{cases} \tag{1.32}$$ {EGo}

DiWa84

Ultimately, we will be interested in the radiation intensity at a detector loction $\boldsymbol{r}$ that is far away from the scattering target. We expand for $r \gg r'$:

$$\left|\boldsymbol{r}-\boldsymbol{r}'\right| \doteq \sqrt{r^2-2\boldsymbol{r}\,\boldsymbol{r}'} \doteq r - \frac{\boldsymbol{r}\,\boldsymbol{r}'}{r} \equiv r - \frac{\boldsymbol{k}_\mathrm{f}\boldsymbol{r}'}{K}, \tag{1.33}$$ {Effa}

where we have introduced the outgoing wavevector $\boldsymbol{k}_\mathrm{f} \coloneqq K\hat{\boldsymbol{r}}$. We define the projection operator

$$\boldsymbol{P} = \begin{cases} 1 & \text{for neutrons (scalar),} \\ \mathbf{1} & \text{for neutrons (spinorial),} \\ \mathbf{1}-\hat{\boldsymbol{k}}_\mathrm{f}\otimes\hat{\boldsymbol{k}}_\mathrm{f} & \text{for X-rays.} \end{cases} \tag{1.34}$$ {EdefP}

With this, we find the far-field asymptote of the Green function,

$$\boldsymbol{G}_0^\infty(\boldsymbol{r},\boldsymbol{r}') = \boldsymbol{P}g(r)\mathrm{e}^{-i\boldsymbol{k}_\mathrm{f}\boldsymbol{r}'}. \tag{1.35}$$ {EGoInfty}

1.2.3 Differential cross section

The differential scattering cross section is defined as

$$\frac{\mathrm{d}\sigma}{\mathrm{d}\Omega} \coloneqq \frac{r^2 J_\mathrm{f}(\boldsymbol{r})}{J_\mathrm{i}}. \tag{1.36}$$ {E1xsectiondef}

With fluxes given by (1.22) and with the scattered far-field denoted as in Sec. 1.2.1,

$$\frac{\mathrm{d}\sigma}{\mathrm{d}\Omega} = \frac{r^2|\boldsymbol{\Psi}_\mathrm{s}^\infty(\boldsymbol{r})|^2}{|\boldsymbol{\Phi}_\mathrm{i}|^2}. \tag{1.37}$$ {E1xsectiondef}

At this point, we choose the incident $\boldsymbol{\Phi}_\mathrm{i}$ to be a normalized plane wave

$$\boldsymbol{\Phi}_\mathrm{i}(\boldsymbol{r}) = (2\pi)^{-3/2}\hat{\boldsymbol{u}}_\mathrm{i}\mathrm{e}^{i\boldsymbol{k}_\mathrm{i}\boldsymbol{r}}. \tag{1.38}$$ {EPlaneIn}

We combine (1.29), (1.35) and (1.38) to find

$$\boldsymbol{\Psi}_\mathrm{s}^{\infty}(\boldsymbol{r}) = g(r)\boldsymbol{P}\boldsymbol{V}(\boldsymbol{q})\hat{\boldsymbol{u}}_\mathrm{i} \tag{1.39}$$ {E1PsiS2}

with the Fourier transformed potential

$$\boldsymbol{V}(\boldsymbol{q}) = \int \mathrm{d}^3r\, \mathrm{e}^{-i\boldsymbol{q}\boldsymbol{r}}\boldsymbol{V}(\boldsymbol{r}) \tag{1.40}$$

and the scattering vector[2]

$$\boldsymbol{q} \coloneqq \boldsymbol{k}_\mathrm{f} - \boldsymbol{k}_\mathrm{i}. \tag{1.41}$$ {Eq}

With all this, the cross section (1.37) becomes

$$\frac{\mathrm{d}\sigma}{\mathrm{d}\Omega} = \frac{1}{16\pi^2}\left\langle \hat{\boldsymbol{u}}_\mathrm{i}\boldsymbol{V}^{+}(\boldsymbol{q})\boldsymbol{P}\boldsymbol{V}(\boldsymbol{q})\hat{\boldsymbol{u}}_\mathrm{i}\right\rangle. \tag{1.42}$$ {Exsection}

1.2.4 X-ray cross section and polarization factor

In the electromagnetic case, per Sec. 1.1.3 and (1.19), we only consider scalar potentials. There is, however, a nontrivial projector $\boldsymbol{P}$ (1.34) that ensures transversality. In consequence, the cross section (1.37) can be written

$$\frac{\mathrm{d}\sigma}{\mathrm{d}\Omega} = \frac{1}{16\pi^2}\tilde{P}|\boldsymbol{V}(\boldsymbol{q})|^2 \tag{1.43}$$ {ExsectionX}

with the polarization factor

$$\tilde{P} \coloneqq \hat{\boldsymbol{u}}_\mathrm{i}\boldsymbol{P}\hat{\boldsymbol{u}}_\mathrm{i} = 1 - (\hat{\boldsymbol{k}}_\mathrm{f}\hat{\boldsymbol{u}}_\mathrm{i})^2. \tag{1.44}$$

It will be evaluated later, when we discuss grazing-incidence and reflectometry geometry.

1.2.5 Neutron cross section and polarization analysis

For neutrons, the projector $\boldsymbol{P}$ (1.34) is just the identity matrix, and therefore can be omitted from the cross section (1.37). In the absence of magnetic scattering, the potential is scalar, and the cross section is simply

$$\frac{\mathrm{d}\sigma}{\mathrm{d}\Omega} = \frac{1}{16\pi^2}|V(\boldsymbol{q})|^2. \tag{1.45}$$ {ExsectionN}

In the presence of magnetic scattering, additional insight can be gained by polarization analysis of the scattered radiation. If the polarization analyzer is set in direction $\hat{\boldsymbol{u}}_\mathrm{f}$, then instead of (1.42) one finds

$$\frac{\mathrm{d}\sigma}{\mathrm{d}\Omega} = \frac{1}{16\pi^2}|\hat{\boldsymbol{u}}_\mathrm{i}\boldsymbol{V}(\boldsymbol{q})\hat{\boldsymbol{u}}_\mathrm{f}|^2. \tag{1.46}$$ {ExsectionN}

[2] With this choice of sign, $\hbar\boldsymbol{q}$ is the momentum *gained* by the scattered neutron, and *lost* by the sample. In much of the literature the opposite convention is prefered, since it emphasizes the sample physics over the scattering experiment. However, when working with two-dimensional detectors it is highly desirable to express pixel coordinates and scattering vector components with respect to equally oriented coordinate axes, which can only be achieved by the convention (1.75).

1.3 Distorted-wave Born approximation

As we have seen in the preceding Sec. 1.2, the Born approximation leads to particularly simple results when applied to the scattering of plane waves. Under grazing incidence, however, refraction and reflection often distort the incoming and the scattered wave in ways that cannot be accounted for by perturbative scattering theory. One rather needs to compute these distortions by analytical or numerical means, then apply the Born approximation to the so obtained distorted wave fronts. This is called the *distorted-wave Born approximation* (DWBA).[3]

1.3.1 Distortion versus perturbation

To get started, we decompose the potential (1.19) into a more regular and a more fluctuating part:

$$\boldsymbol{V}(\boldsymbol{r}) =: \boldsymbol{\Lambda}(\boldsymbol{r}) + \boldsymbol{U}(\boldsymbol{r}). \tag{1.47}$$ {Edecompose}

The *distortion field* $\boldsymbol{\Lambda}$ comprises regular, well-known features of the sample. The *perturbation potential* $\boldsymbol{U}$ stands for the more irregular, unknown features of the sample one ultimately wants to study in a scattering experiment. This is vague, and in certain situations the decomposition (1.47) is indeed to some extent arbitrary. In our application context, $\boldsymbol{\Lambda}(z)$ is responsible for refractions and reflections by multilayer structures, whereas $\boldsymbol{U}(\boldsymbol{r})$ accounts for all lateral fluctuations.

The distortion field $\boldsymbol{\Lambda}$ is combined with the vacuum wave operator $\boldsymbol{D}_0$ (1.18) into the *distorted wave operator*

$$\boldsymbol{D}(\boldsymbol{r}) \coloneqq \boldsymbol{D}_0 - \boldsymbol{\Lambda}(\boldsymbol{r}) \tag{1.48}$$ {EdefD}

that governs the unperturbed distorted wave equation

$$\boldsymbol{D}(\boldsymbol{r})\boldsymbol{\Phi}(\boldsymbol{r}) = 0. \tag{1.49}$$ {EDPsi0}

The solutions $\boldsymbol{\Phi}$ are the *distorted* waves that are scattered by the perturbation $\boldsymbol{U}$, as developed below in Sect. 1.3.3. SxDWBA

[3] The DWBA was originally devised by Massey and Mott (ca 1933) for collisions of charged particles. Summaries can be found in some quantum mechanics textbooks (Messiah, Schiff) and in monographs on scattering theory (e. g. Newton). The first explicit applications to grazing-incidence scattering were published in 1982: Vineyard [11] discussed X-ray scattering, but failed to account for the distortion of the scattered wave; Mazur and Mills [12] deployed heavy formalism to compute the inelastic neutron scattering cross section of ferromagnetic surface spin waves from scratch. A concise derivation of the DWBA cross section was provided by Dietrich and Wagner (1984/85) for X-rays [13] and neutrons [14]. Unfortunately, their work was overlooked in much of the later literature, which often fell back to less convincing derivations. Vin82 MaMi82 Diwa84 Diwa85

1.3.2 Refractive index

Except for neutrons in a magnetic field the distortion field is scalar so that it can be expressed through the *refractive index*

$$n(\boldsymbol{r}) \coloneqq \sqrt{1-\frac{4\pi\Lambda(\boldsymbol{r})}{K^2}} = \begin{cases} \sqrt{1-4\pi\overline{v}(\boldsymbol{r})/K^2} & \text{for neutrons,} \\ \sqrt{\epsilon(\boldsymbol{r})} & \text{for X-rays.} \end{cases} \tag{1.50}$$ {EnkK}

If $\overline{v}(\boldsymbol{r})$ or $\epsilon(\boldsymbol{r})$ has an imaginary part, describing absorption, then $n(\boldsymbol{r})$ is a complex number. Conventionally, n is parameterized by two real numbers:

$$n =: 1-\delta+i\beta. \tag{1.51}$$ {Endb1}

Appendix A explains how to determine δ and β.

For thermal neutrons and X-rays, with quantum-mechanical sign convention [(1.2) and (1.12)], δ and β are almost always nonnegative, and much smaller than 1. This explains why in most scattering geometries the ordinary Born approximation with $\boldsymbol{\Lambda} \equiv 0$ is perfectly adequate. In layered samples under grazing incidence, however, even small differences in n can cause substantial refraction and reflection. To model GISAS, therefore, it is necessary to use DWBA, and to let $\boldsymbol{\Lambda}$ represent the average vertical refractive index profile $\overline{n}(z)$.

1.3.3 Scattering cross section in DWBA

With the conventions (1.47) and (1.48), we rewrite the wave equation (1.17) of the full, perturbed problem as

$$(\boldsymbol{D}-\boldsymbol{U})\,|\boldsymbol{\Psi}\rangle = 0. \tag{1.52}$$ {EWave3}

It is solved in perfect analogy with Sec. 1.2.1. In place of (1.25), we have the Lippmann-Schwinger equation

$$|\boldsymbol{\Psi}\rangle = |\boldsymbol{\Phi}_\mathrm{i}\rangle + \boldsymbol{G}\boldsymbol{U}\,|\boldsymbol{\Psi}\rangle \tag{1.53}$$ {ELS3}

with the distorted-wave Green function

$$\boldsymbol{G} \coloneqq \boldsymbol{D}^{-1} \tag{1.54}$$ {EdefG}

and with $|\boldsymbol{\Phi}_\mathrm{i}\rangle$ now designating a distorted incident wave. In analogy with (1.28), the scattered wave far away from the sample is

$$|\boldsymbol{\Psi}_\mathrm{s}^{\infty}\rangle \coloneqq \boldsymbol{G}^{\infty}\boldsymbol{U}\,|\boldsymbol{\Phi}_\mathrm{i}\rangle\,. \tag{1.55}$$ {EBornS}

1.3.4 The DWBA far-field Green function

From Sec. 1.3.3, the task is left over to determine the far-field Green function $\boldsymbol{G}^{\infty}$. Assume we know the Green function of the undistorted wave equation **??**,

$$\boldsymbol{G}_0 \coloneqq \boldsymbol{D}_0^{-1}. \tag{1.56}$$ {EdefG0}

Write the distorted wave equation **??** as a Lippmann-Schwinger equation

$$|\boldsymbol{\Phi}\rangle = |\boldsymbol{k}\alpha\rangle + \boldsymbol{G}_0\boldsymbol{U}\,|\boldsymbol{\Phi}\rangle\,. \tag{1.57}$$ {ELS2}

To verify, operate with $\boldsymbol{D}_0$ from the left. Solve formally through simple algebraic manipulations,

$$|\boldsymbol{\Phi}\rangle = (\mathbf{1} - \boldsymbol{G}_0\boldsymbol{U})^{-1}\,|\boldsymbol{k}\alpha\rangle =: \boldsymbol{R}\,|\boldsymbol{k}\alpha\rangle\,. \tag{1.58}$$ {EPhi}

DiWa84,DiWa85,DiWa16

Following Dietrich and Wagner [13, 14, 15], we note that the distorted-wave Green function (1.54) also obeys a Lippmann-Schwinger equation,

$$\boldsymbol{G} = \boldsymbol{G}_0 + \boldsymbol{G}_0\boldsymbol{U}\boldsymbol{G}. \tag{1.59}$$

To verify, operate again with $\boldsymbol{D}_0$ from the left. Resolve algebraically for

$$\boldsymbol{G} = (\mathbf{1} - \boldsymbol{G}_0\boldsymbol{U})^{-1}\boldsymbol{G}_0 \equiv \boldsymbol{R}\boldsymbol{G}_0. \tag{1.60}$$

To make use of (1.59), we insert a complete projector,

$$\boldsymbol{G} = \sum_{\alpha}\int \mathrm{d}^3k\,\boldsymbol{R}\,|\boldsymbol{k}\alpha\rangle\,\langle\boldsymbol{k}\alpha|\,\boldsymbol{G}_0 = \sum_{\alpha}\int \mathrm{d}^3k\;|\boldsymbol{\Phi}_{\boldsymbol{k}\alpha}\rangle\,\langle\boldsymbol{k}\alpha|\,\boldsymbol{G}_0 \tag{1.61}$$

where the dependence of $\boldsymbol{\Phi}$ on the boundary condition $\boldsymbol{k}\alpha$ is explicitly denoted. As $\boldsymbol{G}_0$ is known in real-space representation, we insert another projector,

$$\boldsymbol{G} = \sum_{\alpha}\int \mathrm{d}^3k \int \mathrm{d}^3r''\;|\boldsymbol{\Phi}_{\boldsymbol{k}\alpha}\rangle\,\langle\boldsymbol{k}\alpha|\boldsymbol{r}''\rangle\,\langle r''|\,\boldsymbol{G}_0. \tag{1.62}$$

In real-space coordinates,

$$\boldsymbol{G}(\boldsymbol{r},\boldsymbol{r}') = (2\pi)^{-3}\sum_{\alpha}\int \mathrm{d}^3k \int \mathrm{d}^3r''\,\boldsymbol{\Phi}_{\boldsymbol{k}\alpha}(\boldsymbol{r})\otimes\hat{\boldsymbol{u}}_{\alpha}\mathrm{e}^{-i\boldsymbol{k}\boldsymbol{r}''}\boldsymbol{G}_0(\boldsymbol{r}'',\boldsymbol{r}'). \tag{1.63}$$ {EGrspace}

At this point, we need the vacuum Green function $\boldsymbol{G}_0$.

We apply reciprocity **??** to **????** and insert the resulting

$$\boldsymbol{G}_0^{\infty}(\boldsymbol{r},\boldsymbol{r}') = \mathbf{1}\psi_{\mathrm{f}}^{*}(\boldsymbol{r})g(r') \tag{1.64}$$

into (1.64) to obtain

$$\lim_{r'\to\infty}\boldsymbol{G}(\boldsymbol{r},\boldsymbol{r}') = \sum_{\alpha}\boldsymbol{\Phi}_{\boldsymbol{k}_{\mathrm{f}}\alpha}(\boldsymbol{r})\otimes\hat{\boldsymbol{u}}_{\alpha}g(r'). \tag{1.65}$$ {EGresult}

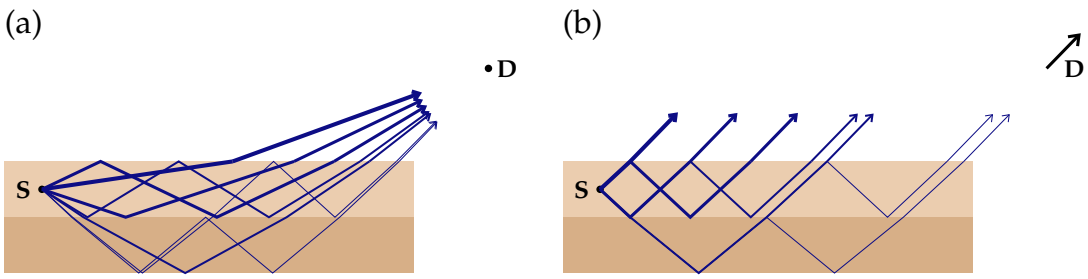

Figure 1.1: (a) The Green function $G(\boldsymbol{r}_\mathrm{S}, \boldsymbol{r}_\mathrm{D})$ is the probability that radiation emitted by a source S is reaches a detector D. If S is a locus of scattering in a multilayer sample, then G is a sum over different trajectories, involving refraction and reflection at layer interfaces. (b) For the far-field Green function $G^\infty(\boldsymbol{r}_\mathrm{S}, \boldsymbol{r}_\mathrm{D})$, the detector is moved so far away from the sample that all trajectories are practically parallel when they leave the sample.

1.3.5 Reciprocity of the Green function

Our computation of G_∞ will be based on a source-detector *reciprocity theorem* for the scalar Schrödinger equation.[4] The theorem states: Any Green function $G(\boldsymbol{r}, \boldsymbol{r}')$ that solves **??** and as function of $\boldsymbol{r}$ represents an outgoing wave is invariant under an exchange of source location $\boldsymbol{r}_\mathrm{S}$ and detection point $\boldsymbol{r}_\mathrm{D}$:

$$G(\boldsymbol{r}_\mathrm{S}, \boldsymbol{r}_\mathrm{D}) = G(\boldsymbol{r}_\mathrm{D}, \boldsymbol{r}_\mathrm{S}). \tag{1.66}$$ {Erecip}

Readers not interested in mathematical details may skip the following *proof*:

We introduce the auxiliary vector field

$$\boldsymbol{X}(\boldsymbol{r}, \boldsymbol{r}_\mathrm{S}, \boldsymbol{r}_\mathrm{D}) \coloneqq G(\boldsymbol{r}, \boldsymbol{r}_\mathrm{D})\boldsymbol{\nabla} G(\boldsymbol{r}, \boldsymbol{r}_\mathrm{S}) - G(\boldsymbol{r}, \boldsymbol{r}_\mathrm{S})\boldsymbol{\nabla} G(\boldsymbol{r}, \boldsymbol{r}_\mathrm{D}). \tag{1.67}$$

We inscribe the sample and the detector into a sphere $\mathcal{S}$ around the coordinate origin with radius R, and compute the volume integral

$$I(\boldsymbol{r}_\mathrm{S}, \boldsymbol{r}_\mathrm{D}) \coloneqq \int_\mathcal{S} \mathrm{d}^3 r\, \boldsymbol{\nabla} \boldsymbol{X}(\boldsymbol{r}, \boldsymbol{r}_\mathrm{S}, \boldsymbol{r}_\mathrm{D}). \tag{1.68}$$ {Eprerecipro}

After a few steps, not entirely trivial, but not too difficult either, we obtain

$$I(\boldsymbol{r}_\mathrm{S}, \boldsymbol{r}_\mathrm{D}) = G(\boldsymbol{r}_\mathrm{S}, \boldsymbol{r}_\mathrm{D}) - G(\boldsymbol{r}_\mathrm{D}, \boldsymbol{r}_\mathrm{S}). \tag{1.69}$$ {EIBD}

Alternatively, we can compute I as a surface integral

$$I(\boldsymbol{r}_\mathrm{S}, \boldsymbol{r}_\mathrm{D}) = \int_{\partial\mathcal{S}} \mathrm{d}\boldsymbol{\sigma}\, \boldsymbol{X}(\boldsymbol{r}, \boldsymbol{r}_\mathrm{S}, \boldsymbol{r}_\mathrm{D}). \tag{1.70}$$

[4] There exists a confusing multitude of reciprocity theorems [16]. In the end, we found it simpler to provide a derivation taylored for our application case than to refer to the literature.

On the surface $\partial\mathcal{S}$, G is an outgoing solution of the Helmholtz equation. As such, it has a well-known series expansion in spherical coordinates. We send $R \to \infty$ so that we need only to retain the lowest order:

$$G(\boldsymbol{r}(R,\vartheta,\varphi),\boldsymbol{r}_{\mathrm{D}}) \doteq \frac{\mathrm{e}^{iKR}}{4\pi R} a(\vartheta,\varphi), \tag{1.71}$$

$$G(\boldsymbol{r}(R,\vartheta,\varphi),\boldsymbol{r}_{\mathrm{S}}) \doteq \frac{\mathrm{e}^{iKR}}{4\pi R} b(\vartheta,\varphi). \tag{1.72}$$

The factorization of G and B and their common R dependence imply that

$$I(\boldsymbol{r}_{\mathrm{S}},\boldsymbol{r}_{\mathrm{D}}) = \int_{\partial\mathcal{S}} \mathrm{d}\sigma\, (R\text{-dependent})(ab - ba) = 0. \tag{1.73}$$

Comparison with (1.70) yields (1.67), which completes the proof.

OLD STUFF

exciting vs incident wave

The solution of the wave equation **??** starts with the determination of the incident wave $\boldsymbol{\Psi}_\mathrm{i}$. It is important to distinguish the *incident* from the *exciting* wave. They coincide in ordinary Born approximation, but not in DWBA.

The *exciting wave* is prepared far outside the sample by a radiation source and some optical devices. It is a superposition of plane waves, as discussed later in the context of instrumental resolution effects (**??**). Here we will consider a single plane wave $\boldsymbol{\Psi}_\mathrm{e}(\boldsymbol{r}) = \hat{\boldsymbol{u}}_\mathrm{e} e^{i\boldsymbol{k}_\mathrm{e}\boldsymbol{r}}$. This function is defined for all $\boldsymbol{r}$, but is physical only along the primary beam, upstream of the sample.

The *incident wave* $\boldsymbol{\Psi}_\mathrm{i}$ is an exact solution of (1.49) under the boundary condition that it match $\boldsymbol{\Psi}_\mathrm{e}$ upstream of the sample. Inside the sample it undergoes refraction and reflection or other modifications under the influence of the distortion field $\boldsymbol{\Lambda}$.

Scattering vector q

the *scattering vector*[5]

$$\boldsymbol{q} \coloneqq \boldsymbol{k}_\mathrm{f} - \boldsymbol{k}_\mathrm{i}. \tag{1.74}$$ {Eq}

[5] With this choice of sign, $\hbar\boldsymbol{q}$ is the momentum *gained* by the scattered neutron, and *lost* by the sample. In much of the literature the opposite convention is prefered, since it emphasizes the sample physics over the scattering experiment. However, when working with two-dimensional detectors it is highly desirable to express pixel coordinates and scattering vector components with respect to equally oriented coordinate axes, which can only be achieved by the convention (1.75).

1.4 Coherent vs incoherent scattering

1.4.1 Density operator

An eigenfunction of the vacuum wave operator $\boldsymbol{D}_0$ is a plane wave with real wavevector $\boldsymbol{k}$. In the spinor or vector case, its polarization shall be expressed in an orthonormal base $\{\boldsymbol{u}_\alpha\}$ with $\alpha = 1, 2$ (for spin 1/2 or for traverse electric field in vacuum). The corresponding eigenstate can be written as ket $|\boldsymbol{k}\alpha\rangle$, the real-space coordinate representation as

$$\boldsymbol{\Psi}_{\boldsymbol{k}\alpha}(\boldsymbol{r}) \equiv \langle \boldsymbol{r}|\boldsymbol{k}\alpha\rangle = (2\pi)^{-3/2}\boldsymbol{u}_\alpha \mathrm{e}^{i\boldsymbol{k}\boldsymbol{r}}. \tag{1.75}$$ {EvacWave}

The incident neutron beam in an actual scattering experiment is not such a *pure* state, but a statistical mixture of states, and must therefore be described by the density operator

$$\boldsymbol{\rho} \coloneqq \sum_{\boldsymbol{k}\alpha} p_{\boldsymbol{k}\alpha} \left|\boldsymbol{k}\alpha\right\rangle \left\langle \boldsymbol{k}\alpha\right|, \tag{1.76}$$ {EdefRho}

where $p_{\boldsymbol{k}\alpha}$ quantifies the contribution of pure state $|\boldsymbol{k}\alpha\rangle$.

1.4.2 Coherence length

Per (1.42) and **??**, the matrix element $\langle\psi_\mathrm{i}|\delta v|\psi_\mathrm{f}\rangle$ is given by a three-dimensional integral

$$\langle\psi_\mathrm{i}|\delta v|\psi_\mathrm{f}\rangle \coloneqq \int \mathrm{d}^3 r\, \psi_\mathrm{i}^*(\boldsymbol{r})\delta v(\boldsymbol{r})\psi_\mathrm{f}(\boldsymbol{r}). \tag{1.77}$$ {Etrama3}

The integration domain is effectively limited to a finite z interval, where $\delta v(\boldsymbol{r})$ is nonzero. The horizontal integration domain, however, is infinite within our formalism, which is of course an idealization. Obviously, physical integration limits are imposed by the finite *illuminated sample area*.[6] Another limitation comes from the finite *coherence length* of the instrumental setup, which usually is much shorter than the sample width and length [17, 18].[7] MaPR10, MaMM14

While each single neutron is described by a wavefunction that allows for *coherent* superposition of different contributions to the scattered wavefunction, the final detector statistics is given by an *incoherent* sum over the differential cross sections of individual neutrons. The finite *resolution* of an experimental setup is in part due to the fact that different neutrons have different wavenumbers, originate[8] at different points in the moderator, and are detected at slightly different points within one detector pixel.

[6] We assume a well aligned instrument, for which the beam footprint and the backtracked detector footprint agree within reasonable accuracy.

[7] These two references also make clear that the theoretical description and the experimental determination of coherence lengths are difficult problems and subject of ongoing research.

[8] It is reasonable to take the last collision in the moderator as the *origin* of a neutron ray, since collisions between neutrons and hydrogen nuclei bound in disordered matter lead to almost perfect decoherence.

This can be modeled by computing expected scattering intensities as averages over different neutrons with K, $\hat{\boldsymbol{k}}_\mathrm{i}$, and $\hat{\boldsymbol{k}}_\mathrm{f}$ drawn at random from appropriate distributions.

However, this is not the full story. In the above introduction to the Born approximation we have made the standard assumption that an incoming neutron can be described by a plane wave $\psi_\mathrm{i} = \mathrm{e}^{i\boldsymbol{k}_\mathrm{i}\boldsymbol{r}}$. The wavefunction ψ_f traced back from the detector is also approximated by a plane wave. In the DWBA we allow these waves to be distorted within the sample, but when impinging on the sample they still are plane. A plane wave obviously is an idealized concept, since it has infinite lateral extension. The *transverse coherence length* indicates the scale beyond which this approximation becomes invalid. At larger scales, the wave fronts appear randomly distorted. Physical causes of these distortions include reflections in the neutron guide, diffraction by guide windows and other slits, and diffraction by imperfect monochromator crystals. Of course the distorted wave still admits a Fourier decomposition into plane waves with slightly different wavevectors. In practice, it is impossible to distinguish this spread of wavevectors from the incoherent spread described in the previous paragraph. The instrumental resolution function therefore accounts for both causes of wavevector distortion.

Usually, therefore, a GISANS image is an incoherent average over coherent diffraction patterns collected from many small subareas of the sample. Only horizontal sample structures on scales smaller the coherence length yield interference patterns. Structure fluctuations on larger scales produce said incoherent average of different GISANS images.

The crossover from coherent to incoherent scattering is of course a gradual one. The coherence length indicates where a certain, somewhat arbitrary degree of decoherence is reached. Under these reservations one defines a *coherence spot* in the cross section of an approximately plane wave as an area where the coherence is above a certain threshold. Unless the wave has been prepared in a highly anisotropic guide and slit system, this spot is about circular. Under grazing incidence conditions however, the projection of this spot onto the sample surface yields a very elongated ellipse. Therefore, the coherence length is much larger in x than in y or z direction.[9]

1.4.3 Implementation

Unless otherwise said, BornAgain simulates *coherent* diffraction patterns obtained by the linear superposition of scattered waves. To simulate an *incoherent* mixture of diffraction patterns, the most generic solution is a script with an outer loop that averages over several coherent computations with appropriately distributed parameters.

Currently, BornAgain does not support interferences between particles in different layers.

[9] This has nothing to do with the distinction of *transverse* and *longitudinal* coherence length. Longitudinal coherence has to do with wavelength stability and is of no importance for elastic scattering. We are talking here about *horizontal* and *vertical* projections of the *transverse* coherence length.

A Refractive Indexes for Neutrons and X-Rays

A.1 Introduction

For both, neutrons and X-rays, the refractive index n is defined as (1.51)

$$n \equiv 1 - \delta + i\beta. \tag{A.1}$$

where δ and β are defined in a different way for neutrons and X-rays.

A.2 Calculation for neutrons

For unpolarized neutrons, δ and β are calculated in a following way [19]:

$$\delta = \frac{Nb\lambda^2}{2\pi}, \quad \beta = \frac{N\alpha_a\lambda}{4\pi} \tag{A.2}$$ {eq:deltabeta}

where N is the atomic number density, b is the coherent scattering length, λ is the neutron wavelength, α_a is the absorption cross-section. Nb is also called neutron scattering length density (SLD) and can be calculated using the online calculators. b and α_a are to be found in tables [20]. N is calculated as

$$N = \frac{N_a}{V} \tag{A.3}$$

where $N_a = 6.022 \times 10^{23}$ mol^{-1} is the Avogadro constant and V is the molar volume (cm^3/mol) evaluated as:

$$V = \frac{M}{\rho} \tag{A.4}$$

Here M is the molar mass (g/mol) of the material and ρ is the mass density (g/cm^3). It is important to mention, that for the complex materials, M, b and α_a are calculated as a sum of those for the compounds. α_a in the table [20] is given for the neutron velocity of 2200 m/s and must be recalculated for the considered λ. For this recalculation assumption that $\alpha_a \propto 1/v$, where v is the neutron velocity, is used. Since $v \propto 1/\lambda$, for the given wavelength one can use the following expression:

$$\alpha_a(\lambda) = \alpha_a(2200 \text{ m/s}) \cdot \frac{\lambda}{1.798} \tag{A.5}$$

where λ is the wavelength in Å and 1.798 Å is the wavelength corresponding to the neutron velocity of 2200 m/s.

Example. In the following example we calculate the δ and β for the GaAs using the aforementioned expressions. Molar masses can be taken from the periodic table.

$$\begin{aligned} M_{Ga} &= 69.723 \text{ g/mol} \\ M_{As} &= 74.921595 \text{ g/mol} \\ M_{GaAs} &= M_{Ga} + M_{As} \\ \rho_{GaAs} &= 5.32 \text{ g/cm}^3 \end{aligned}$$

Incoherent scattering lengths and absorption cross-sections are taken from the table [20].

$$\begin{aligned} b_{Ga} &= 7.288 \times 10^{-13} \text{ cm} \\ b_{As} &= 6.58 \times 10^{-13} \text{ cm} \\ b_{GaAs} &= b_{Ga} + b_{As} \\ \alpha_a(Ga) &= 2.75 \times 10^{-24} \text{ cm}^2 \\ \alpha_a(As) &= 4.5 \times 10^{-24} \text{ cm}^2 \\ \alpha_a(GaAs) &= \alpha_a(Ga) + \alpha_a(As) \end{aligned}$$

Let's consider that $\lambda = 12$ Å. For this wavelength, the $\alpha_a(GaAs)$ is recalculated as

$$\alpha_a(GaAs, 12 \text{ Å}) = \alpha_a(GaAs) \cdot \frac{12}{1.798} = 48.38179 \times 10^{-24} \text{ cm}^2$$

Finally, using these values in the equation (A.2), we obtain

$$\begin{aligned} \delta &= 7.04 \times 10^{-5} \\ \beta &= 1.0233 \times 10^{-8} \end{aligned}$$

Comment. For the case of absorption processes included, δ and β may be expressed in the following form [21]:

$$\delta = \frac{\lambda^2 N}{2\pi}\sqrt{b^2 - \left(\frac{\sigma_r}{2\lambda}\right)^2}, \qquad \beta = \frac{\sigma_r N \lambda}{4\pi} \tag{A.6}$$

where $\sigma_r = \alpha_a + \sigma_i$ is the sum of the absorption and incoherent scattering cross sections.

A.3 Case of polarized neutrons

For the spin-polarized neutrons scattered on the magnetic multilayers, the magnetic scattering length b_m must be taken into account. It can be expressed in the form [22] WiCa09

$$b_m = 1.913 e^2 S / m_e \tag{A.7}$$

where S is the spin of the magnetic atom in the direction perpendicular to the momentum transfer $\mathbf{q}$ and e and m_e are the charge and mass, respectively, of the electron. The total coherent scattering length is then

$$b_{\text{total}} = b_{\text{nuclear}} \pm b_m \tag{A.8}$$

where the sign $\pm$ corresponds to the beam being polarized parallel or antiparallel to the magnetization direction of the sample [22]. Values for magnetic scattering lengths can be found in tables [23, 5, 21, 20, 24]. WiCa09 KoRS91,Sea92,RaWa00,Sea92online,RaWa00Online

A.4 Calculation for X-rays

In the case of X-rays scattering originates from the strong variations of the mean electronic density as a homogeneous medium does not scatter [25]. Thus, the dispersion δ and absorption contribution β are expressed in the following form [25].

$$\delta(\mathbf{q},\lambda) = \frac{e^2\lambda^2}{8\pi^2 m_e c^2 \varepsilon_0} \cdot \rho \cdot \frac{\sum \left[f_k^0(\mathbf{q},\lambda) + f_k'(\lambda)\right]}{\sum M_k} \tag{A.9}$$

$$\beta = \frac{e^2\lambda^2}{8\pi^2 m_e c^2 \varepsilon_0} \cdot \rho \cdot \frac{\sum f_k''(\lambda)}{\sum M_k} \tag{A.10}$$

where c is the speed of light, ε_0 is the permittivity constant, M_k is the atomic weight of the atom k, and f_k' and f_k'' are the dispersion corrections [25] or atomic scattering factors [26]. The summation is performed over all compound atoms k. For the very high photon energies, f_k^0 approaches Z_k^*, which is expressed as [26]:

$$Z_k^* = Z_k - \left(\frac{Z_k}{82.5}\right)^{2.37} \tag{A.11}$$

where Z_k is the atomic number. Tables for the atomic scattering factors can be found in [26]. There are online calculators for the refractive indexes available in [27].

Bibliography

PoHB20 [1] G. Pospelov, W. Van Herck, J. Burle, J. M. Carmona Loaiza, C. Durniak, J. M. Fisher, M. Ganeva, D. Yurov and J. Wuttke, J. Appl. Cryst. **53**, 262 (2020). vi, vii, 1:1, 1:2

Laz06 [2] R. Lazzari, *IsGISAXS*. Version 2.6. http://www.insp.jussieu.fr/oxydes/IsGISAXS/isgisaxs.htm (2006). vii

Laz02 [3] R. Lazzari, J. Appl. Cryst. **35**, 406 (2002). vii

ReLL09 [4] G. Renaud, R. Lazzari and F. Leroy, Surf. Sci. Rep. **64**, 255 (2009). vii, 1:3

Sea92 [5] V. P. Sears, Neutron News **3**, 26 (1992). 1:2, A:4, X:2

Sea89 [6] V. P. Sears, *Neutron Optics*, Oxford University Press: Oxford (1989). 1:2

Mez86 [7] F. Mezei, Physica B+C **137**, 295 (1986). 1:2

MaOB06 [8] C. F. Majkrzak, K. V. O'Donovan and N. F. Berk, in *Neutron Scattering from Magnetic Materials*, edited by T. Chatterji, Elsevier: Amsterdam (2006). 1:2

Lau31 [9] M. v. Laue, Erg. exakt Naturwiss. **10**, 133 (1931). 1:3

Sch14 [10] H. Schober, J. Neutron Res. **17**, 109 (2014).

Vin82 [11] G. H. Vineyard, Phys. Rev. B **26**, 4146 (1982). 1:8

MaMi82 [12] P. Mazur and D. L. Mills, Phys. Rev. B **26**, 5175 (1982). 1:8

DiWa84 [13] S. Dietrich and H. Wagner, Z. Phys. B **56**, 207 (1984). 1:6, 1:8, 1:10

DiWa85 [14] S. Dietrich and H. Wagner, Z. Phys. B **59**, 35 (1985). 1:8, 1:10

DiWa16 [15] S. Dietrich and H. Wagner, *Private communication* (2016). 1:10

Pot04 [16] R. J. Potton, Rep. Progr. Phys. **67**, 717 (2004). 1:11

HaPR10 [17] V. O. de Haan, J. Plomp, M. T. Rekveldt, A. A. van Well, R. M. Dalgliesh, S. Langridge, A. J. Böttger and R. Hendrikx, Phys. Rev. B **81**, 094112 (2010). 1:14

MaMM14 [18] C. F. Majkrzak, C. Metting, B. B. Maranville, J. A. Dura, S. Satja, T. Udovic and N. F. Berk, Phys. Rev. A **89**, 033851 (2014). 1:14

Mue13 [19] P. Müller-Buschbaum, Polym. J. **45**, 34 (2013). A:2

2online [20] NIST Center for Neutron Research, *Neutron scattering lengths and cross sections according to [5]*, *http://www.ncnr.nist.gov/resources/n-lengths/list.html*. A:2, A:3, A:4

RaWa00 [21] H. Rauch and W. Waschkowski, in *Landolt-Börnstein - Group I Elementary Particles, Nuclei and Atoms 16A1 (Low Energy Neutrons and their Interaction with Nuclei and Matter. Part 1)*, edited by H. Schopper (2000). A:3, A:4, X:2

WiCa09 [22] B. T. M. Willis and C. J. Carlile, *Experimental neutron scattering*, Oxford University Press: Oxford (2009). A:4

KoRS91 [23] L. Koester, H. Rauch and E. Seymann, Atom. Data Nucl. Data **49**, 65 (1991). A:4, X:2

0online [24] Atominstitut der österreichischen Universitäten, *Neutron scattering lengths and cross sections according to [23, 21]*, *http://www.ati.ac.at/~neutropt/scattering/table.html*. A:4

Mue09 [25] P. Müller-Buschbaum, in *Applications of Synchrotron Light to Scattering and Diffraction in Materials and Life Sciences*, edited by M. Gomez, A. Nogales, M. C. Garcia-Gutierrez and T. A. Ezquerravolume 776 of *Lect. Notes Phys.* (Lect. Notes Phys. 776) (2009). A:5

HeGD93 [26] B. L. Henke, E. M. Gullikson and J. C. Davis, Atom. Data Nucl. Data **54**, 181 (1993). A:5, X:2

3online [27] Lawrence Berkeley National Laboratory, Materials Sciences Division, Center for X-Ray Optics, *X-Ray Interactions With Matter. Online calculators based on [26]*. *http://henke.lbl.gov/optical_constants*. A:5

List of Symbols

β	Imaginary part of the refractive index, 1:7
δ	Small parameter in the refractive index $n = 1 - \delta + i\beta$, 1:7
ϵ_0	Vacuum permittivity, 8.854…As/Vm, 1:3
$\epsilon(\boldsymbol{r})$	Relative dielectric permittivity function, 1:3
$\boldsymbol{\epsilon}(\boldsymbol{r})$	Relative dielectric permittivity tensor, 1:3
$\boldsymbol{\Lambda}(\boldsymbol{r})$	Distortion field, 1:6
μ	Absolute value of the magnetic moment of the neutron, $1.91\mu_{\mathrm{N}}$, 1:2
$\boldsymbol{\mu}(\boldsymbol{r})$	Relative magnetic permeability tensor, 1:3
$\hat{\rho}$	Density operator, 1:4
$\rho(\boldsymbol{r})$	Electron number density, 1:3
ρ_s	Number density of chemical element s, 1:2
σ	Scattering or absorption cross section, 1:8
$\boldsymbol{\sigma}$	Pauli vector, composed of the three Pauli matrices: $\boldsymbol{\sigma} = (\sigma_x, \sigma_y, \sigma_z)$, 1:2
$\psi(\boldsymbol{r})$	Stationary wavefunction, 1:1
$\psi(\boldsymbol{r}, t)$	Microscopic neutron wavefunction, 1:1
$\psi_{\mathrm{s}}(\boldsymbol{r})$	Scattered wavefunction, 1:8
$\boldsymbol{\Psi}_{\mathrm{i}}(\boldsymbol{r})$	Incident wavefunction, 1:11
$\boldsymbol{\Psi}_{\mathrm{e}}(\boldsymbol{r})$	Exciting wave, 1:11
$\boldsymbol{\Psi}(\boldsymbol{r})$	Generic wave amplitude, possibly vectorial or spinorial, 1:4
ω	Frequency of incident radiation, 1:1
Ω	Solid angle, 1:8
b	Bound scattering length, 1:2

$\boldsymbol{B}(\boldsymbol{r},t)$	Magnetic field, 1:3
$\boldsymbol{D}_0(\boldsymbol{r})$	Differential operator in the vacuum wave equation, 1:4
$\boldsymbol{D}(\boldsymbol{r})$	Differential operator in the wave equation, 1:6
$\boldsymbol{D}(\boldsymbol{r},t)$	Displacement field, 1:3
$\boldsymbol{E}(\boldsymbol{r},t)$	Electric field, 1:3
f	Subscript "final", 1:5
$\boldsymbol{G}(\boldsymbol{r},\boldsymbol{r}')$	Generic (possibly tensorial) Green function, 1:7
$\boldsymbol{G}^{\infty}(\boldsymbol{r},\boldsymbol{r}')$	Far-field approximation to the Green function $G(\boldsymbol{r},\boldsymbol{r}')$, 1:9
$\boldsymbol{b}(\boldsymbol{r})$	Rescaled field $\boldsymbol{b} = (m\mu/2\pi\hbar^2)\boldsymbol{B}$, 1:3
$\boldsymbol{B}(\boldsymbol{r},t)$	Magnetic induction, 1:2
i	Subscript "incident", 1:11
$\boldsymbol{J}(\boldsymbol{r})$	Flux, 1:5
$\boldsymbol{k}$	Wavevector, 1:4
K	Wavenumber in vacuum, 1:1
n	Refractive index, 1:7
$p_{\boldsymbol{k}\alpha}$	Weight of state $ket\boldsymbol{k}\alpha$ in the density operator, 1:4
$\boldsymbol{q}$	Scattering vector, 1:11
r_e	Classical electron radius $2.817\ldots^{-15}$ m, 1:3
$\boldsymbol{r}$	Position, 1:1
$\boldsymbol{r}_{\mathrm{D}}$	Position of detector, 1:10
$\boldsymbol{r}_{\mathrm{D}}$	Position of source, locus of scattering, 1:10
s	Subscript "scattered", 1:8
$\boldsymbol{S}$	Poyinting vector, 1:5
t	Time, 1:1
$\boldsymbol{U}(\boldsymbol{r})$	Perturbation potential, 1:6
$v(\boldsymbol{r})$	Rescaled neutron potential, scattering length density (SLD), 1:2
$V(\boldsymbol{r})$	Neutron potential, 1:1
$\boldsymbol{V}(\boldsymbol{r})$	Generic potential, 1:4

Index